Journal of Engineering Science *Vol. XXXI, no. 4 (2024), pp. 124 - 141*
Fascicle *Electronics and Computer Science* *ISSN 2587-3474*
Topic *Computers and Information Technology* *eISSN 2587-3482*

https://doi.org/10.52326/jes.utm.2024.31(4).09
UDC 681.515:004.4:621.865.8

CASCADE CONTROL ALGORITHM OF THE ROBOTIC ARM'S SERVOMOTOR

Dumitru Moraru *, ORCID: 0000-0001-8957-6046,
Ion Fiodorov, ORCID: 0000-0003-0938-3442,
Bartolomeu Izvoreanu, ORCID: 0000-0001-9886-5878,
Irina Cojuhari, ORCID: 0000-0003-2248-1338

Technical University of Moldova, 168 Stefan cel Mare Blvd., Chisinau, Republic of Moldova
* Corresponding author: Dumitru Moraru, dumitru.moraru@ati.utm.md

Received: 12. 02. 2024
Accepted: 12. 28. 2024

Abstract. In this paper, there have been synthesized the control algorithms in cascade control systems. The control object is the robotic arm which is actuated by a servo motor presented as an automatic cascade control system which is consisting of two loops. The use of multiple loops is justified by the fact that with a single loop, only one parameter of the servo motor is controlled, which leads to a decrease in the reliability of the automatic system. A case study was carried out for a direct current electric motor, where proportional (P), proportional-integral (PI), and proportional-integral-derivative (PID) control algorithms were used, with P and PI applied to the inner loop, and P, PI, and PID to the outer loop. The system was simulated with the synthesized algorithms and the results were analyzed, it was established that the system has robustness and high performance for the case of using maximum stability degree method with iterations.

Keywords: *maximum stability degree method with iterations, proportional-integral-derivative controller, automatic control system, cascade control systems.*

Rezumat. În lucrare sunt sintetizați algoritmii din cadrul sistemelor de reglare în cascadă. Obiectul de reglare este brațul robotic acționat de un servomotor, prezentat ca un sistem automat de reglare în cascadă format din două bucle. Utilizarea mai multor bucle este argumentată de faptul că, într-un sistem cu o singură buclă, doar un singur parametru al servomotorului poate fi reglat, ceea ce duce la o scădere a fiabilității sistemului automat. A fost realizat un studiu de caz pentru un motor electric de curent continuu, unde au fost utilizați algoritmi de reglare proporțional (P), proporțional-integrativ (PI) și proporțional-integrativ-derivativ (PID), cu P și PI aplicate pentru bucla interioară și P, PI și PID pentru bucla exterioară. Sistemul a fost simulat utilizând algoritmii sintetizați, iar rezultatele au fost analizate, stabilindu-se că sistemul are robustețe și performanțe ridicate în cazul utilizării metodei gradului maxim de stabilitate cu iterații.

Cuvinte cheie: *metoda gradului maximal de stabilitate cu iterații, regulator proporțional-integrativ-derivativ, sistem de reglare automat, sistem de reglare în cascadă.*

1. Introduction

In recent decades, robots have passed a fast way in their evolution, one of the main stages being the emergence of soft (flexible) robots. For actions such as grasping and manipulating with objects, soft (flexible) robots realize much better with the passive adaptation required due to unpredictability and changing environmental conditions. In other words, while a rigid robot must be programmed in advance to capture an object, a soft robot can do it on its own due to passive adaptation [1-3].

Although soft robotics technology has evolved in terms of mobility, tactile perception is much more important for extending the manipulative capabilities of robots [4].

Tactile perception in robotics often faces problems of non-linearity, low receptor density and/or lack of modularity, which prevents the adoption of a single solution. Distributed data arrays obtained by tactile sensors address the low-density problem to some extent, but they are usually limited to flexible boards or soft sensors with strongly non-linear characteristics. Currently, the main challenge in this field lies in the development of sensor models that can provide high-precision information for closed-loop control [1-5].

At the same time, the perception of touching the object by the robot can be realized by following the parameters of the execution element, such as voltage, current of direct current (DC) motors, servomotors etc. [5-8].

The servomotor is a commonly used as actuator element in the construction of robotic arms due to its ability to provide precise positioning of the position of the arm or part of the robot. A servo motor is a type of electric motor specifically designed to provide precise positioning in a mechanical system. The field of use includes: robotic arms, robots, computer numerical control (CNC) machines, aircraft, automobiles, industrial equipment, medicine etc. [7, 8].

2. Problem formulation

Given the mathematical model of a DC servomotor with permanent magnets, it is described the second order with astatism transfer function [9-13]:

$$H_M(s) = \frac{k}{s(T_m T_e s^2 + T_m s + 1)}, \quad (1)$$

where: k is transfer coefficient, T_m – electromechanical time constant, T_e – electrical time constant.

In order to verify the hypothesis, that a single control loop of the servo output shaft angle is not enough, a DC motor model with known parameters was used:

Maximum rotor voltage $U_r = 6$ V.

Power $P = 0.46$ W.

Nominal rotations $n_n = 2850$ rpm.

Rotor current $I_r = 0.076$ A.

Engine torque $M_m = 0.0016$ Nm.

The active resistance of the rotor $R = 7.9\ \Omega$.

The moment of inertia of the motor $J_m = 0.91 \cdot 10^{-7}$ kgm^2.

The transfer coefficient k represents the rotor voltage - angular speed of the motor and is calculated based on the technical data by the expression:

$$k = \frac{1}{k_e} = \frac{n}{U_r - \alpha R I_r} = \frac{2850}{6 - 1.2 \cdot 7.9 \cdot 0.076} = 539.77 \text{ (rpm/V)}.$$

It is calculated the coefficient k_e by the relation:

$$k_e = \frac{1}{k} = \frac{1}{539.77} = 0.00185.$$

The electromechanical time constant is calculated according to the relationship:

$$T_m = \frac{1}{9.55}\frac{J\alpha R}{k_m k_e} = \frac{1}{9.55}\frac{0.91\cdot 10^{-7}\cdot 1.2\cdot 7.9}{0.0176\cdot 0.00185} = 0.00277 \text{ s}.$$

The coefficient k_m it is calculated by the expression:

$$k_m = \frac{k_e}{0.105} = \frac{0.00185}{0.105} = 0.0176.$$

Inductance with $\beta = 0.3$ and $p = 2$ poles it is calculated by the relations:

$$L = \frac{30}{\pi}\beta\frac{U_r}{pnI_R} = \frac{30}{3.14}0.3\frac{6}{2\cdot 2850\cdot 0.076} = 0.03969 \text{ H}.$$

The electrical time constant T_e is calculated by the relation:

$$T_e = \frac{L}{R} = \frac{0.03968}{7.9} = 0.00502 \text{ s}.$$

The coefficients are introduced in (1) and it is obtained the motor transfer function:

$$H_M(s) = \frac{k}{T_m T_e s^2 + T_m s + 1} = \frac{539.77}{0.00277\cdot 0.00502 s^2 + 0.00277 s + 1} = \\ = \frac{539.77}{1.39\cdot 10^{-5} s^2 + 0.00277 s + 1}.$$

In the motor coil the current changes according to the equivalent transfer function of a simple inductor [8]:

$$H_I(s) = \frac{U_{\text{int}}}{Ls + R} = \frac{4.5}{0.003968s + 7.9}, \tag{2}$$

where: $H_I(s)$ is the transfer function of the current change in the motor coil (rotor), U_{int} − the voltage applied to the coil which must not exceed the maximum admissible voltage (6 V) for the supply, L − the inductance of the coil and R − the resistance of the coil.

Due to the fact that astatism is present in the system (which occurs because the rotations of the DC motor need to be converted into angular displacement) the P controller was chosen as a simple solution and closer to the real object that was tuned using parametric optimization.

As mentioned above, the motor supply voltage is 4.5 V, from this reason a saturation element with limits between -4.5 and +4.5 V was introduced in the structural block diagram of the system (Figure 1) [14].

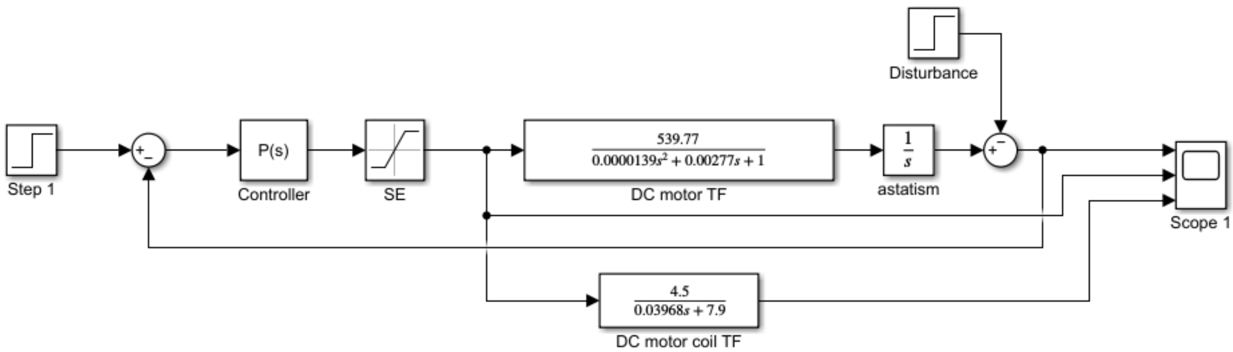

Figure 1. Structural block scheme of the automatic control system with one loop.

Figure 2 depicts the index step response of the automatic control system (curve 1), the voltage applied to the motor generated by the controller P (curve 2) and the variation of the current in the motor coil (curve 3).

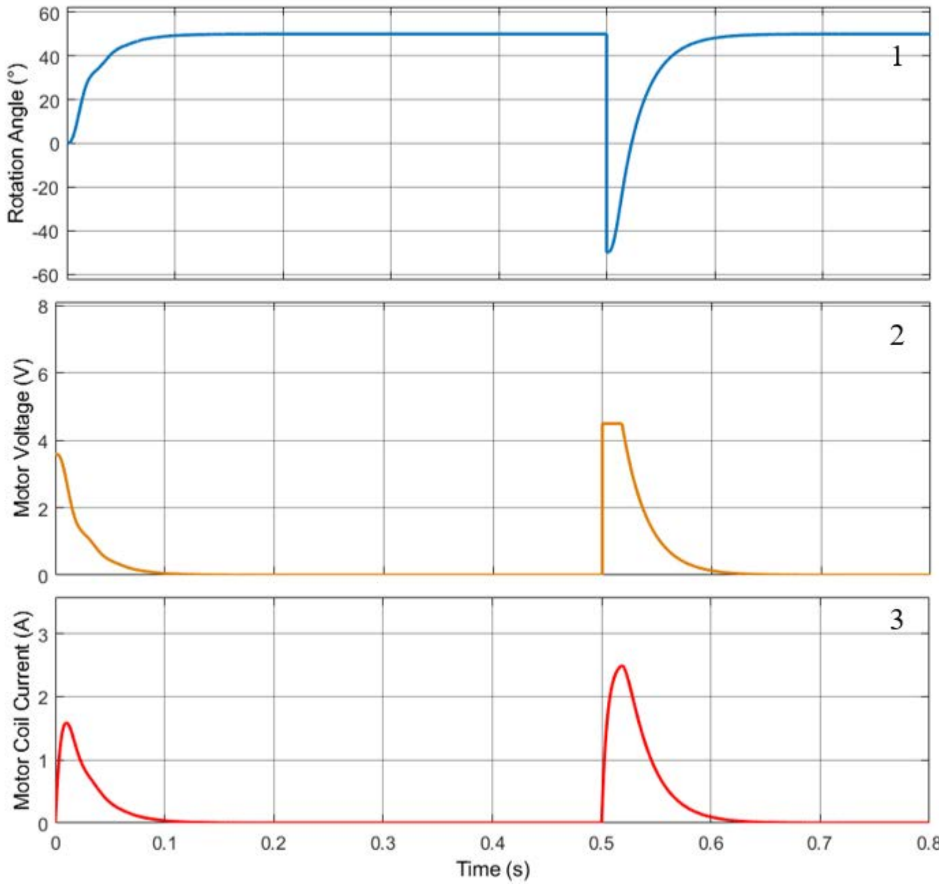

Figure 2. The response of the control system to the step signal with the application of the disturbance.

Analyzing the curves from Figure 2, can be observed that a sudden increase the current in the motor coil, both when the system is started and when the load disturbance is applied at 0.5 s from start-up. According to the technical data of the motor, the maximum current of the motor coil is 0.076 A, and on the transient process a peak of about 2 A is observed at system start-up and about 2.5 A at the moment of applying the disturbance, which is approximate 33 times greater the rated current. The duration for which the current exceeding the allowed limit is approximately 0.1 s for the case of applying the load disturbance, during which the power transistors fail to dissipate the amount of heat dissipate and often go out of commission, motor coils usually hold up because they have a greater ability to dissipate power on itself.

In order to make the control of the servomotors more efficient, the system with two loops is proposed to use. The inner loop performs the control of the motor coil current, and the outer loop control the rotation angle of the servo motor.

3. Synthesis automatic control algorithms for system with two control loops

Cascade control structures are used for control fast and slow processes with or without time delay. The presence of many time constants in the transfer function of the fixed part makes it difficult to use some typical control algorithms, which impose the compensation of these time constants, by control algorithms containing several first-degree binomials. There are given difficulties in the tuning of such control algorithms, taking into account the negative effect that derivative components have on the system response (amplification of noises) it is recommended to use cascade control structures. The structural block scheme of the two-loop automatic control system with servomotor is represented in Figure 3 [15-23].

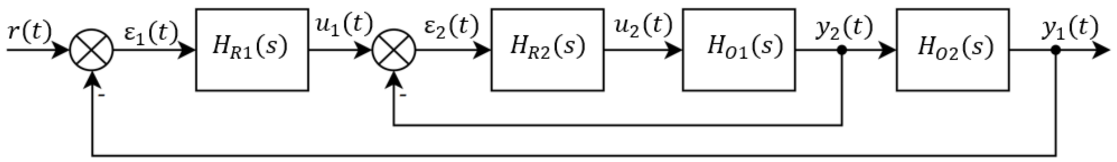

Figure 3. Structural block –scheme of the two-loop automatic control system.

Tuning the controllers in cascade control systems is done from the inner loop and then it is performed in the outer loop.

Figure 4 presents the structural block scheme of the DC motor for controlling the rotation angle.

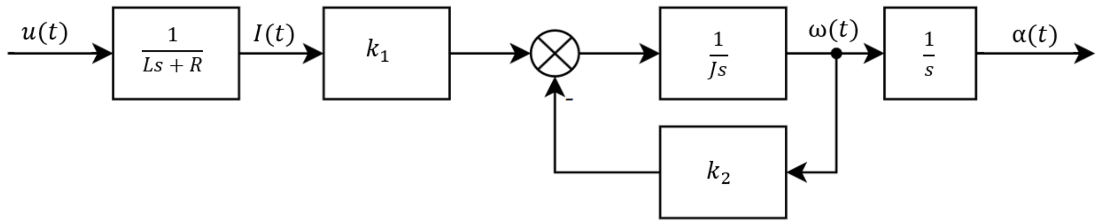

Figure 4. Structural block scheme of the DC motor.

In Figure 4, the following notations are used: $u(t)$ is the command signal (supply voltage), $\frac{1}{Ls+R}$ – the transfer function of the electromechanical component (coil) of the motor, k_1– the torque coefficient of the motor, $\frac{1}{Js}$ – the transfer function of the mechanical component of the engine, k_2 – the viscous friction force coefficient, $\omega(t)$ – the angular speed of the rotor and $\alpha(t)$ – the rotation angle of the rotor shaft.

According to the structural block scheme of the DC motor, the expressions for the parts $H_{01}(s)$ and $H_{02}(s)$ of the control object are following:

$$H_{01}(s) = \frac{k_2}{Ls+R} = \frac{539.77}{0.03968s+7.9}, \quad (3)$$

$$H_{02}(s) = \frac{\frac{1}{Js}}{1+\frac{1}{Js}k_3}\frac{1}{s} = \frac{1}{Js+k_3}\frac{1}{s} = \frac{1}{0.91\cdot10^{-7}s^2+0.002s}, \quad (4)$$

A. Tuning the controller in the inner loop

In the inner loop, it is recommended to use controllers with a simpler structure than in the outer one. Next, the synthesis of the P and PI controllers are presented according to the maximum stability degree method (MSD). PD and PID controllers cannot be tuned by the MSD method, because according to the methodology of the MSD method, the order of the characteristic equation of the closed loop system must be greater than or equal to the number of tuned parameters [24,25].

It is considered the inner loop represented in Figure 5.

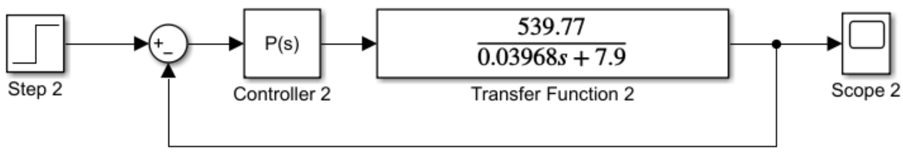

Figure 5. Structural block scheme of the inner loop.

The procedure of tuning P and PI controllers consists from following steps:

1. It is chosen one of the desired control laws.
2. The transfer function of the closed loop system with the chosen control algorithm is obtained.
3. The characteristic equation of the closed loop is obtained.
4. The substitution $p =- J$ in the characteristic equation is done.
5. Derivation on variable J of the characteristic equation from point 4 is performed a number of times equal to the number of tuning parameters.
6. From the equation obtained in point 5, its roots are determined, which represent the degrees of stability of the designed automatic system, and the value of the optimal degree J_{opt} is the smallest real root, or the real part of the complex root.
7. Using J_{opt} and the algebraic equations obtained in step 5, the parameter values of the chosen control laws are calculated.
8. The performance of the designed automatic control system is verified by computer simulation [24,25].

If the system performance is not satisfied by the analytical calculations, it is recommended to use the maximum stability degree method with iterations (MSDI), which consists in determining the analytical expressions of the tuning parameters, that depend on the object's parameters that are known and stability degree parameter, that is unknown and there are obtained the dependencies $k_p = f_p(J)$, $k_i = f_i(J)$.

At the variation of the stability degree J from for the P and PI control algorithms and the sets of values are chosen from the obtained curves of the tuning parameters P and I $J_i - k_{pi}$, k_{ii}. Next, the automatic control system with the chosen control algorithm is simulated on the computer and there are obtained the transient responses, after which the highest possible performance of the system is determined, which would satisfy the imposed performance of the automatic control system.

If the performances of the system are satisfied, the synthesis procedure is finished, or otherwise, the procedure starts from the beginning with another type of control law or another tuning method.

For the calculation of the tuning parameters of the typical P and PI controllers transfer function (3) is presented in a generalized form:

$$H_{01}(s) = \frac{539.77}{0.03968s+7.9} = \frac{k_2}{a_0 s + \mathrm{a}_1}, \tag{5}$$

where $k_2 = 539.77$ is transfer coefficient, and the generic coefficients of the control object are $a_0 = 0.03968$, that represents the time constant of the process and $a_1 = 7.9$.

Synthesis the P controller in the inner loop

The transfer function of inner closed loop with P controller is presented:

$$H_0 = \frac{H_R(s)H_{01}(s)}{1+H_R(s)H_{01}(s)} = \frac{k_{p2}k_2}{a_0 s + a_1 + k_{p2}k} = \frac{B(s)}{A(s)}, \tag{6}$$

where k_{p2} is tuning parameter of the P controller.

The characteristic equation $A(s)$ of the inner loop is:

$$A(s) = a_0 s + a_1 + k_{p2}k = \frac{a_0 s + a_1}{k_2} + k_{p2} = 0. \tag{7}$$

According to the algorithm of maximum stability degree method, it is done the substitution s=−J and it is obtained the expression:

$$A(-J) = \frac{-a_0 J + a_1}{k_2} + k_{p2} = 0. \tag{8}$$

For determining the tuning parameter of the P controller by the MSDI method from expression (8) it is obtained the relation:

$$k_{p2} = \frac{a_0 J - a_1}{k_2} = \frac{0.03968J - 7.9}{539.77}. \tag{9}$$

The variation of J from 0 to 300 means investigating the system's performance at different levels of stability. Figure 6 illustrates the dependency of P controller parameter k_{p2} on the stability degree J.

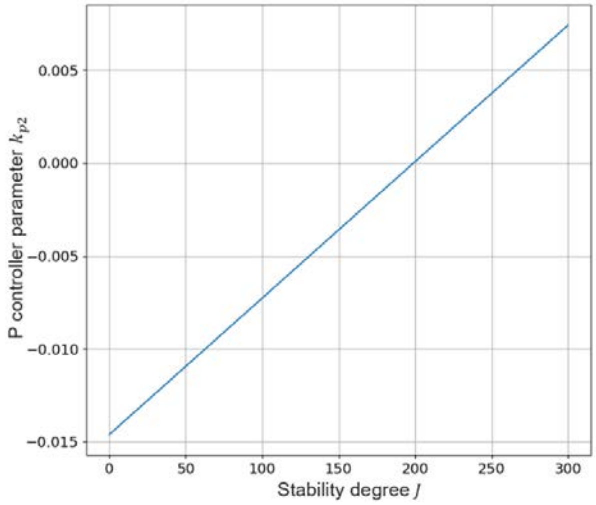

Figure 6. Dependence $\boldsymbol{k_{p2} = f_{p2}(J)}$.

From sets of obtained values $k_{p2} = f_{p2}(J)$, the values that provide the best performance for the automatic control system are selected. Figure 7 depict the transient responses of the system corresponding to different selected values of k_{p2}.

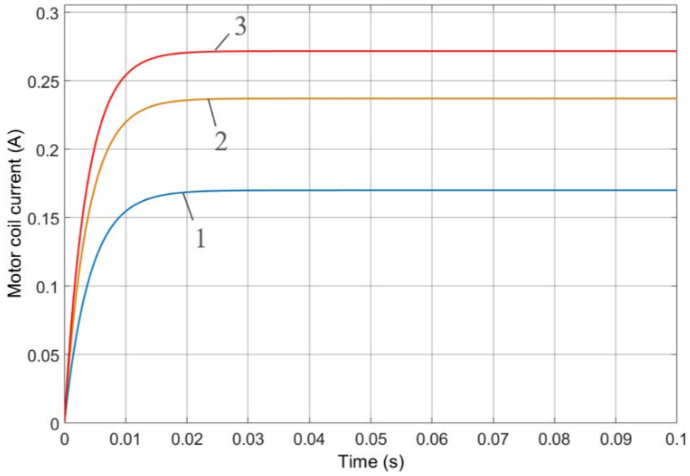

Figure 7. The step response of the inner loop with P controller.

Note: *the transient responses labeled 1, 2 and 3 correspond to the No. iter. listed in Table 1.*

In Table 1, there are presented the performances of the automatic control system of the DC motor coil current with P controller.

In the case of the P controller, the steady-state error is high, because P controller cannot be used in the inner loop.

Table 1

Tuning parameters and performances of the automatic control system with P controller

No. iter.	J	k_{p2}	t_r (s)	σ (%)	t_s (s)	n
1	240	0.003	0.0088	-	0.012	-
2	261	0.00455	0.0095	-	0.011	-
3	273.5	0.00546	0.0091	-	0.011	-

Note: J – stability degree, k_{p2} – P controller parameter, t_r – rise time, σ – overshoot, t_s – settling time, n – number of deviations from the set value.

Synthesis of the PI controller in the inner loop

It is determinate the transfer function of the inner loop with PI controller:

$$H_{0i} = \frac{H_R(s)H_{01}(s)}{1+H_R(s)H_{01}(s)} = \frac{(k_{p2}s+k_{i2})k_2}{a_0s^2+a_1s+(k_{p2}s+k_{i2})k_2} = \frac{B(s)}{A(s)}, \quad (10)$$

where k_{p2}, k_{i2} are tuning parameters of the PI controller.

The characteristic equation $A(s)$ of the system is following:

$$A(s) = s(a_0s + a_1) + (k_{p2}s + k_{i2})k_2 = \frac{a_0s^2+a_1s}{k_2} + k_{p2}s + k_{i2} = 0. \quad (11)$$

According to the algorithm of the MSDI method, it is done the substitution $s = -J$ in expression (11) and after some transformation it is obtained:

$$A(-J) = \frac{a_0J^2-a_1J}{k_2} - k_{p2}J + k_{i2} = 0. \quad (12)$$

In the case of using PI controller, it is necessary to derive equation (12) on the variable J once and there are obtained the expressions:

$$k_{p2} = \frac{2a_0J-a_1}{k_2} = \frac{0.07936J-7.9}{539.77}, \quad (13)$$

$$k_{i2} = \frac{-a_0J^2+a_1J}{k_2} + k_{p2}J = \frac{-0.03968J^2+7.9J}{539.77} + k_{p2}J. \quad (14)$$

At the variation the stability degree value J from 0 to 100, there are calculated and constructed the curves $k_{p2} = f_{p2}(J)$ și $k_{i2} = f_{i2}(J)$ for control algorithm PI (Figure 8).

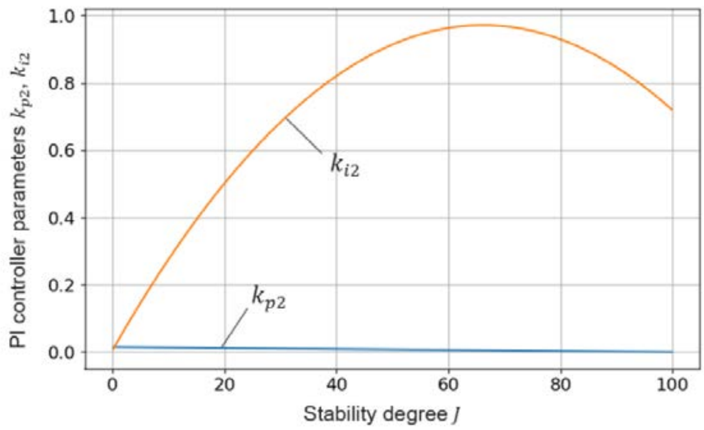

Figure 8. Dependencies $\boldsymbol{k_{p2} = f_{p2}(J)}$ and $\boldsymbol{k_{i2} = f_{i2}(J)}$.

In the Figure 9, there are presented the transient responses of the system for the different values of the k_{p2} and k_{i2}.

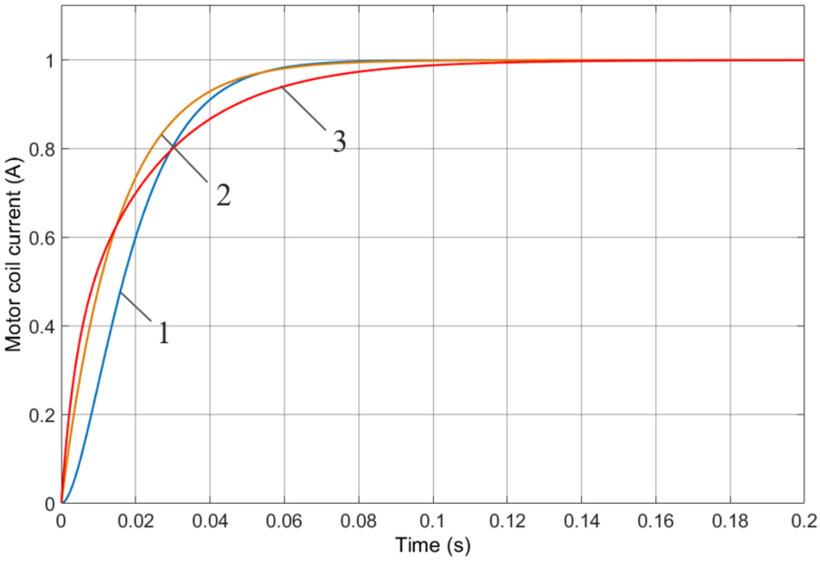

Figure 9. The step response of the inner loop with PI controller.
Note: *the transient responses labeled 1, 2 and 3 correspond to the No. iter. listed in Table 2.*

In Table 2, there are presented the performances of the automatic current control system of the DC motor with PI controller.

In the case of use the PI controller in the inner loop, there are obtained the good performances and the best was obtained for the 3rd iteration from Table 2.

Table 2

Tuning parameters and performances of the automatic control system with PI controller

No. iter.	J	k_{p2}	k_{i2}	T_{i2} (s)	t_r (s)	σ (%)	t_s (s)	n
1	40.5	0.00868	0.8237	1.214	0.041	-	0.047	-
2	66.3	0.00489	0.9713	1.029	0.043	-	0.045	-
3	98.7	0.00012	0.7407	1.35	0.063	-	0.064	-

Note: J – stability degree, k_{p2} – P controller parameter, k_{i2} – I controller parameter, T_{i2} – oscillation period of the I component of controller, t_r – rise time, σ – overshoot, t_s – settling time, n – number of deviations from the set value.

B. Tuning controller in the outer loop

For tuning the controller in the outer loop, it is necessary to calculate the transfer function of the fixed part, which is the product of the transfer function of the closed system $H_0(s)$ from the inner loop $H_{0i}(s)$ and the transfer function of the mechanical component $H_{02}(s)$ of the DC motor. In the inner loop, the PI controller will be used because, following its tuning, the best results were obtained (Table 2, iteration 3).

$$H_0(s) = H_{0i}(s)H_{02}(s) = \frac{(k_{p2}s+k_{i2})k_2}{a_0s^2+a_1s+(k_{p2}s+k_{i2})k_2}\frac{1}{a_2s^2+a_3s} = \frac{c_0s+c_1}{d_0s^4+d_1s^3+d_2s^2+d_3s}, \quad (15)$$

where $c_0 = k_2k_{p2} = 3.9996$, $c_1 = k_2k_{i2} = 892.77$, $d_0 = a_0a_2 = 3{,}61 \cdot 10^{-9}$, $d_1 = a_0a_3 + {}$ $+a_1a_2 + a_2k_{p2}k_2 = 8.044 \cdot 10^{-5}$, $d_2 = a_1a_3 + a_2k_{i2}k_2 + a_3k_{p2}k_2 = 0.0328$ and $d_3 =$ $= a_3k_{i2}k_2 = 1.7855$.

The mathematical model of the control object is with advance first-order, inertia third order and astatism. The structural block scheme of the outer loop of the automatic control system is presented in Figure 10.

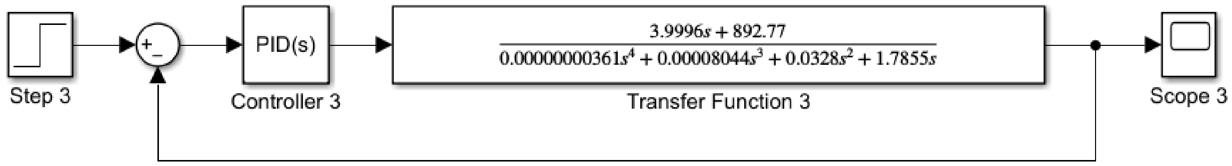

Figure 10. Structural block scheme of the outer loop.

The transfer function of the closed loop system is presented in the following form:

$$H_0(s) = \frac{H_d(s)}{1+H_d(s)} = \frac{H_R(s)H_{PF}(s)}{1+H_R(s)H_{PF}(s)} = \frac{H_R(s)(c_0 s+c_1)}{d_0 s^4+d_1 s^3+d_2 s^2+d_3 s+H_R(s)(c_0 s+c_1)} = \frac{B(s)}{A(s)}, \qquad (16)$$

where $H_d(s) = H_R(s)H_{PF}(s)$ is the transfer function of the open loop system, $H_R(s)$ – transfer function of the controller, where $A(s)$ and $B(s)$ – the system polynomials.

Next, it is presented the procedures for tuning P, PI and PID controllers to the model of object (15).

Synthesis of the P controller in the outer loop

The characteristic equation $A(s)$ of the automatic control system is:

$$A(s) = d_0 s^4 + d_1 s^3 + d_2 s^2 + d_3 s + k_{p1}(c_0 s + c_1) = 0, \qquad (17)$$

where k_{p1} is a tuning parameter of P controller.

According to the algorithm of the MSDI method, it is done the substitution $s = -J$ and after some transformation it is obtained:

$$A(-J) = \frac{d_0 J^4 - d_1 J^3 + d_2 J^2 - d_3 J}{c_1 - c_0 J} + k_{p1} = 0. \qquad (18)$$

In the case of using P controller, it is necessary to derive equation (18) on the variable J once and the following expression is obtained:

$$\dot{D}(-J) = \frac{-3d_0 c_0 J^4 + J^3(4d_0 c_1 + 2d_1 c_0) - J^2(3d_1 c_1 + d_2 c_0) + 2d_2 c_1 J - d_3 c_1}{(c_1 - c_0 J)^2} = 0. \qquad (19)$$

The value of the stability degree J_{opt} is the smallest positive root of the equation:

$$-3d_0 c_0 J^4 + J^3(4d_0 c_1 + 2d_1 c_0) - J^2(3d_1 c_1 + d_2 c_0) + 2d_2 c_1 J - d_3 c_1 = 0. \qquad (20)$$

For determination the tuning parameter of P controller from expression (18) there is used the following relationship:

$$k_{p1} = \frac{-d_0 J^4 + d_1 J^3 - d_2 J^2 + d_3 J}{c_1 - c_0 J} = \frac{3.61 \cdot 10^{-9} J^4 + 8.044 \cdot 10^{-5} J^3 - 0.0328 J^2 + 1.7855 J}{892.77 - 3.9996 J}. \qquad (21)$$

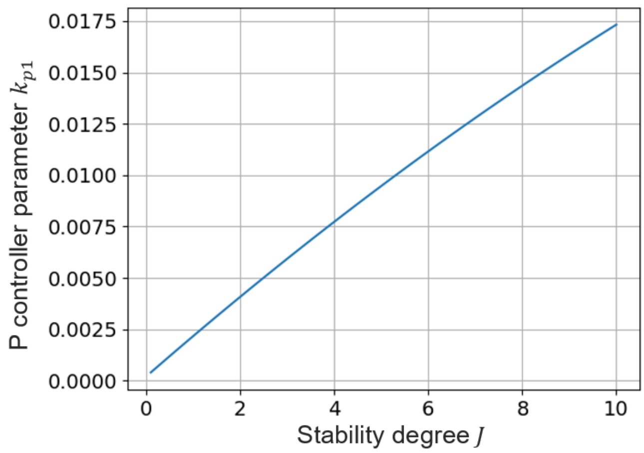

Figure 11. Dependence $k_{p1} = f_{p1}(J)$.

At the variation the stability degree J from 0 to 10, there are calculated and constructed the curves $k_{p1} = f_{p1}(J)$ for the P control algorithm (Figure 11).

In Figure 12, the transient responses of the automatic control system with a P controller in the outer loop are presented for different values of k_{p1}, showing the rotation angle of the servomotor's output shaft.

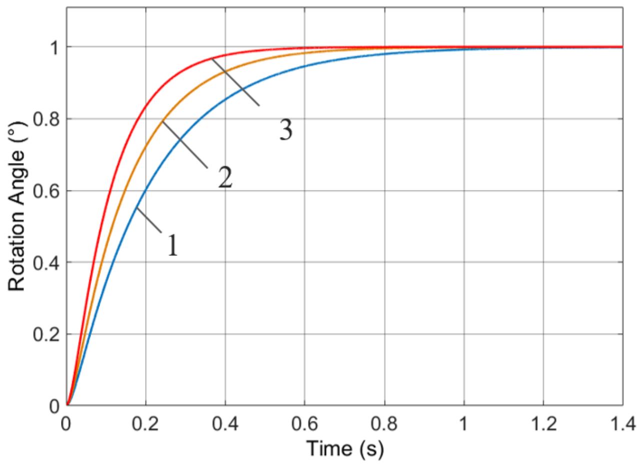

Figure 12. The step response of the outer loop with P controller

Note: *the transient responses labeled 1, 2 and 3 correspond to the No. iter. listed in Table 3.*

Table 3 represents the performance of the automatic control system for controlling the angle of rotation of the servomotor's output shaft with a P controller.

Table 3

Tuning parameters and performances of the automatic control system with P controller

No. iter.	J	k_{p1}	t_r (s)	σ (%)	t_s (s)	n
1	5.0	0.0093	0.579	-	0.615	-
2	7.0	0.0126	0.417	-	0.447	-
3	10.0	0.0175	0.297	-	0.321	**-**

Note: J – stability degree, k_{p1} – P controller parameter, t_r – rise time, σ – overshoot, t_s – settling time, n – number of deviations from the set value.

In the case of the system with P controller in the outer loop, there are obtained the good performances, due to the astatism existing in the object, and the steady-state error is zero (Table 3, iteration 3).

Synthesis of the PI controller in the outer loop

The characteristic equation $A(s)$ of the automatic control system with PI controller is following:

$$A(s) = d_0 s^5 + d_1 s^4 + d_2 s^3 + d_3 s^2 + (k_{p1} s + k_{i1})(c_0 s + c_1) = 0, \quad (22)$$

where k_{p1}, k_{i1} are tuning parameters of PI controller.

According to the algorithm of the MSDI method, it is done the substitution $s = -J$ and after some transformation it is obtained:

$$A(-J) = \frac{-d_0 J^5 + d_1 J^4 - d_2 J^3 + d_3 J^2}{c_1 - c_0 J} - k_{p1} J + k_{i1} = 0. \quad (23)$$

In the case of using PI controller, it is necessary to derive equation (23) on the variable J twice and it is obtained the expression:

$$\ddot{A}(-J) = \frac{d_0 J^6 - d_1 J^5 + d_2 J^4 - d_3 J^3 + d_4 J^2 - d_5 J + d_6}{(c_1 - c_0 J)^4} = 0, \quad (24)$$

where: $d_0 = 12 d_0 c_0^3$, $d_1 = 42 d_0 c_0^2 c_1 + 6 d_1 c_0^3$, $d_2 = 50 d_0 c_0 c_1^2 + 22 d_1 c_0^2 c_1 + 2 d_2 c_0^3$, $d_3 =$ $= 20 d_0 c_1^3 + 28 d_1 c_0 c_1^2 + 8 d_2 c_0^2 c_1$, $d_4 = 12 d_1 c_1^3 + 12 d_2 c_0 c_1^2$, $d_5 = 6 d_2 c_1^3 + 2 d_3 c_0 c_1^2$, $d_6 =$ $= 2 d_3 c_1^3$.

The value of the stability degree J_{opt} is the smallest positive root of the equation:

$$d_0 J^6 - d_1 J^5 + d_2 J^4 - d_3 J^3 + d_4 J^2 - d_5 J + d_6 = 0. \quad (25)$$

For determining the tuning parameters of the PI controller there are used the following relationships:

$$k_{p1} = \frac{4 d_0 c_0 J^5 - J^4 (5 d_0 c_1 + 3 d_1 c_0) + J^3 (4 d_1 c_1 + 2 d_2 c_0) - J^2 (3 d_2 c_1 + d_3 c_0) + 2 d_3 c_1 J}{(c_1 - c_0 J)^2} =$$
$$= \frac{5.77 \cdot 10^{-8} J^5 - 0.000981 J^4 + 0.4783 J^3 - 71.1021 J^2 + 3188.2215 J}{(892.77 - 3.9996 J)^2}, \quad (26)$$

$$k_{i1} = \frac{d_0 J^5 - d_1 J^4 + d_2 J^3 - d_3 J^2}{c_1 - c_0 J} + k_{p1} J =$$

$$= \frac{3.61 \cdot 10^{-9} J^5 - 8.044 \cdot 10^{-5} J^4 + 0.0328 J^3 - 1.7855 J^2}{892.77 - 3.9996 J} + k_{p1} J. \quad (27)$$

At the variation the stability degree J from 0 to 10, there are calculated and constructed the curves $k_{p1} = f_{p1}(J)$ and $k_{i1} = f_{i1}(J)$ for the PI control algorithm (Figure 13).

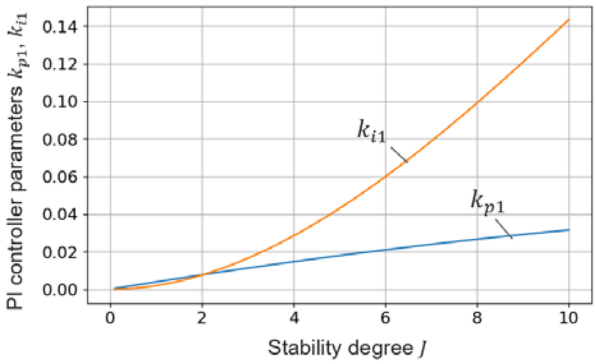

Figure 13. Dependence $\boldsymbol{k_{p1} = f_{p1}(J)}$ and $\boldsymbol{k_{i1} = f_{i1}(J)}$.

In Figure 14 are presented the transient responses of the automatic control system for the different values of k_{p1} and k_{i1}.

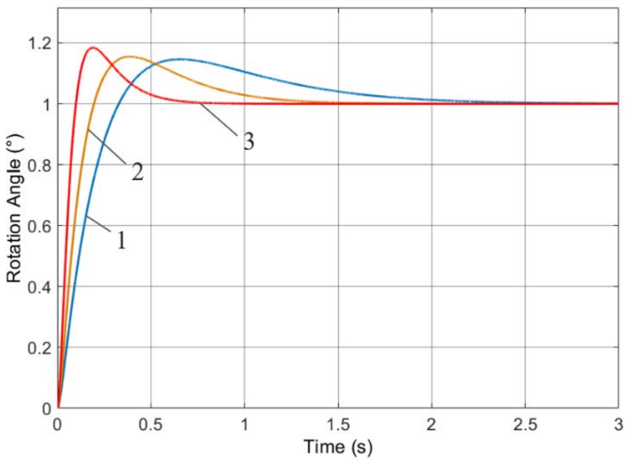

Figure 14. Transient response of the automatic control system with PI controller.
Note: *the transient responses labeled 1, 2 and 3 correspond to the No. iter. listed in Table 4.*

In Table 4 are presented the performance of the automatic control system for controlling the angle of rotation of the servo motor with a PI controller.

Table 4

Tuning parameters and performances of the automatic control system with PI controller

No. iter.	J	k_{p1}	k_{i1}	T_{i1} (s)	t_r (s)	σ (%)	t_s (s)	n
1	3.0	0.01152	0.017	58.82	0.26	14.5	1.4	1
2	5.0	0.01867	0.0455	21.97	0.154	15.4	0.849	1
3	10.0	0.0347	0.1647	6.071	0.075	18.4	0.434	1

Note: J – stability degree, k_{p1} – P controller parameter, k_{i1} – I controller parameter, T_{i1} – oscillation period of the I component of controller, t_r – rise time, σ – overshoot, t_s – settling time, n – number of deviations from the set value.

In the case of the automatic control system with the PI controller in the outer loop, there are obtained the transient processes with overshoot, because of the presence of the astatism component in the system. The best performances were obtained for the 3rd iteration from Table 4.

Synthesis of the PID controller in the outer loop

The characteristic equation $A(s)$ of the automatic control system with PID controller is following:

$$A(s) = d_0 s^5 + d_1 s^4 + d_2 s^3 + d_3 s^2 + (k_{d1} s^2 + k_{p1} s + k_{i1})(c_0 s + c_1) = 0, \quad (28)$$

where k_{p1}, k_{i1}, k_{d1} are tuning parameters of PID controller.

According to the algorithm of the MSDI method, it is done the substitution $s = -J$ and after some transformation it is obtained:

$$A(-J) = \frac{-d_0 J^5 + d_1 J^4 - d_2 J^3 + d_3 J^2}{c_1 - c_0 J} + k_{d1} J^2 - k_{p1} J + k_{i1} = 0. \quad (29)$$

In the case of PID controller it is necessary to derive the expression (29) on the variable J by the three times and there is obtained the following expression:

$$\dddot{A}(-J) = \frac{dJ^9 - \mathrm{d}J^8 + d_2 J^7 - d_3 J^6 + d_4 J^5 - d_5 J^4 + d_6 J^3 - d_7 J^2 + d_8 J - d_9}{(c_1 - \mathrm{c}_0 J)^8} = 0, \quad (30)$$

where $d_0 = 24 d_0 c_0^7$, $d_1 = 186 d_0 c_0^6 c_1 + 6 d_1 c_0^7, d_2 = 624 d_0 c_0^5 c_1^2 + 48 d_1 c_0^6 c_1$, $d_3 = 1176 d_0 c_0^4 c_1^3 + 168 d_1 c_0^5 c_1^2$, $d_4 = 1344 d_0 c_0^3 c_1^4 + 336 d_1 c_0^4 c_1^3$, $d_5 = 930 d_0 c_0^2 c_1^5 + 414 d_1 c_0^3 c_1^4 + 6 d_2 c_0^4 c_1^3 - 6 d_3 c_0^5 c_1^2$, $d_6 = 360 d_0 c_0 c_1^6 + 312 d_1 c_0^2 c_1^5 + 24 d_2 c_0^3 c_1^4 - 24 d_3 c_0^4 c_1^3$, $d_7 = 60 d_0 c_1^7 + 132 d_1 c_0 c_1^6 + 36 d_2 c_0^2 c_1^5 - 36 d_3 c_0^3 c_1^4$, $d_8 = 24 d_1 c_1^7 + 24 d_2 c_0 c_1^6 - 24 d_3 c_0^2 c_1^5$, $d_9 = 6 d_2 c_1^7 - 6 d_3 c_0 c_1^6$.

The optimal value of stability degree J_{opt} is the smallest positive root of the expression:

$$d_0 J^9 - \mathrm{d}_1 J^8 + d_2 J^7 - d_3 J^6 + d_4 J^5 - d_5 J^4 + d_6 J^3 - d_7 J^2 + d_8 J - d_9 = 0. \quad (31)$$

For the calculation tuning parameters of the PID controller there are used the relations:

$$k_p = \frac{4 d_0 c_0 J^5 - J^4 (5 d_0 c_1 + 3 d_1 c_0) + J^3 (4 d_1 c_1 + 2 d_2 c_0) - J^2 (3 d_2 c_1 + d_3 c_0) + 2 d_3 c_1 J}{(c_1 - \mathrm{c}_0 J)^2} + 2 k_{d1} J, \quad (32)$$

$$k_i = \frac{d_0 J^5 - d_1 J^4 + d_2 J^3 - d_3 J^2}{c_1 - c_0 J} - k_{d1} J^2 + k_{p1} J, \quad (33)$$

$$k_d = \frac{-g_0J^6+g_1J^5-g_2J^4+g_3J^3-g_4J^2+g_5J-g_6}{2(c_1-c_0J)^4}, \quad (34)$$

where $g_0 = 12d_0c_0^3$, $g_1 = 42d_0c_0^2c_1 + 6d_1c_0^3$, $g_2 = 50d_0c_0c_1^2 + 22d_1c_0^2c_1 + 2d_2c_0^3$, $g_3 = 20d_0c_1^3 + 28d_1c_0c_1^2 + 8d_2c_0^2c_1$, $g_4 = 12d_1c_1^3 + 12d_2c_0c_1^2$, $g_5 = 6d_2c_1^3 + 2d_3c_0c_1^2$, $g_6 = 2d_3c_1^3$.

At the variation the stability degree value J from 0 to 50, there are calculated and constructed the curves $k_{p1} = f_{p1}(J)$ and $k_{d1} = f_{d1}(J)$ for control algorithm PID (Figure 15).

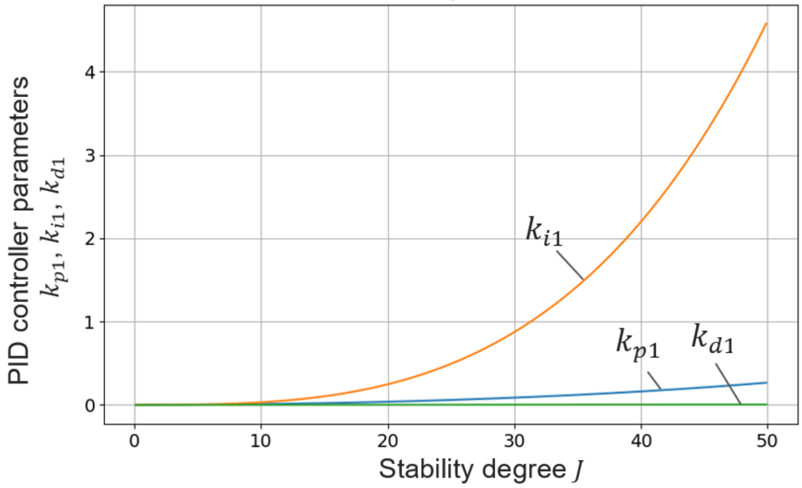

Figure 15. Dependencies $k_{p1} = f_{p1}(J)$, $k_{i1} = f_{i1}(J)$ and $k_{d1} = f_{d1}(J)$.

In the Figure 16 there are presented the transient responses of the automatic control system for the different values of the tuning parameters k_{p1}, k_{i1} and k_{d1}.

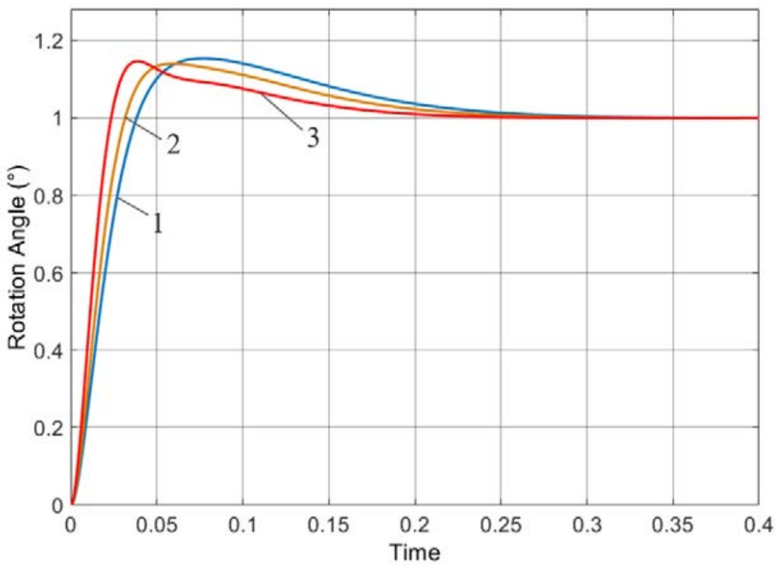

Figure 16. Transient responses of the automatic control system with PID controller.
Note: *the transient responses labeled 1, 2 and 3 correspond to the No. iter. listed in Table 5.*

In Table 5 there are presented the performances of the automatic servo motor rotation angle control system with the PID controller.

For the system with the PID controller in the outer loop, the best performances are presented in Table 5, iteration 3.

Table 5

Tuning parameters and performances of the automatic control system with PID controller

No. iter.	J	k_{p1}	k_{i1}	T_{i1} (s)	k_{d1} (s)	t_r (s)	σ (%)	t_s (s)	n
1	31.8	0.096	1.0387	0.962	0.00092	0.029	15.2	0.182	1
2	34.8	0.1171	1.3865	0.721	0.00123	0.024	14.0	0.158	1
3	40.0	0.1593	2.178	0.459	0.0018	0.017	14.6	0.126	1

Note: J – stability degree, k_{p1} – P controller parameter, k_{i1} – I controller parameter, T_{i1} – oscillation period of the I component of controller, k_{d1} – I controller parameter, t_r – rise time, σ – overshoot, t_s – settling time, n – number of deviations from the set value.

Tuning the controller in the outer loop using the polynomial method

In order to gain a better understanding of the results obtained from tuning the controller using the maximum stability degree method, the polynomial method was used in the outer loop of the DC motor drive system. The synthesis procedure of the control algorithm is reduced to the following steps:

1. The damping ratio is specified $\xi = 0.707$ and the settling time $t_r = 1$ s, and the natural frequency of the outer loop is determined using the following relation:

$$\omega = \frac{4}{\xi t_r} = \frac{4}{0.707 \cdot 1} = 5.658 \text{ s}^{-1}. \qquad (35)$$

2. The dominant poles of the outer loop are determined using the following relation:

$$p_{1,2} = -\xi\omega \pm j\omega\sqrt{1-\xi^2} = -4 \pm j4. \qquad (36)$$

3. According to the polynomial method, the transfer function of the fixed part (15) of degree $n = 4$ of the outer loop is represented in the form:

$$H_0(s) = \frac{c_0 s + c_1}{d_0 s^4 + d_1 s^3 + d_2 s^2 + d_3 s} = \frac{c_0 s + c_1}{s(d_0 s^3 + d_1 s^2 + d_2 s + d_3)} = \frac{C^-(s)C^+(s)}{D^-(s)D^+(s)}, \qquad (37)$$

where: $C^-(s) = c_0 s + c_1$, $C^+(s) = 1$, $D^-(s) = d_0 s^3 + d_1 s^2 + d_2 s + d_3$, $D^+(s) = s$ and we denote the degrees of the respective polynomials: $n_{C^-} = 1$, $n_{C^+} = 0$, $n_{D^-} = 3$, $n_{D^+} = 1$.

4. The desired characteristic polynomial is constructed using the following relation:

$$P_d(s) = C^+(s)M(s) + D^+(s)N(s)s^r, \qquad (38)$$

where: $M(s)$ and $N(s)$ are unknown polynomials that will be determined, and the component s^r introduces astatism (in this case, the degree of astatism is $r = 0$ because the astatism is contained in the fixed part).

The degrees of the polynomials are denoted $P_d(s)$, $M(s)$ and $N(s)$ n_P, n_M, n_N. The coefficients of the polynomials $M(s)$ and $N(s)$ are determined from the system of algebraic equations, which are obtained by equating the coefficients of the same powers on both sides of the polynomial equation (38).

5. The degree of the characteristic polynomial is determined $P_d(s)$ from the condition $n_P == n = 4$. For a simpler implementation of the control algorithm, the smallest values of the degrees n_M, n_N of the unknown polynomials are determined. It is assumed $n_M = 0$ and the degree of n_N is determined from the conditions:

$$n_P \le n_M + n_N + 1, n_N = n_P - n_M - 1 = 4 - 0 - 1 = 3 \qquad (39)$$

and to satisfy these conditions, the values of the unknown degrees are obtained $n_M = 0$ $n_N = 3$. The unknown polynomials are presented in the form:

$$M(s) = m_0, N(s) = n_0 s^3 + n_1 s^2 + n_2 s + n_3. \tag{40}$$

6. The desired characteristic polynomial of the outer loop is constructed using the following relation:

$$P_d(s) = C^+(s)M(s) + D^+(s)N(s) = 1 \cdot m_0 + s(n_0 s^3 + n_1 s^2 + n_2 s + n_3) = \\ = n_0 s^4 + n_1 s^3 + n_2 s^2 + n_3 s + m_0. \tag{41}$$

7. The characteristic polynomial of degree $n = 4$ is constructed based on the dominant poles:

$$P_{dd}(s) = (s + 4 - j4)(s + 4 - j4)(s + 30)^2 = s^4 + 68s^2 + +1412s + 9120s + 28800.$$

8. The polynomials $P_d(s) = P_{dd}(s)$ are equated, and the system of algebraic equations is constructed by equating the coefficients of the same powers of s on both sides:

$$n_0 s^4 + n_1 s^3 + n_2 s^2 + n_3 s + m_0 = s^4 + 68s^2 + +1412s + 9120s + 28800, \\ n_0 = 1, n_1 = 68, n_2 = 1412, n_3 = 9120, m_0 = 28800.$$

9. The transfer function of the controller is constructed using the following relation:

$$H_R(s) = \frac{Q(s)}{P(s)} = \frac{D^-(s)M(s)}{C^-(s)N(s)} = \frac{(d_0 s^3 + d_1 s^2 + d_2 s + d_3)m_0}{(c_0 s + c_1)(n_0 s^3 + n_1 s^2 + n_2 s + m_0)} = \frac{q_0 s^3 + q_1 s^2 + q_2 s + q_3}{p_0 s^4 + p_1 s^3 + p_2 s^2 + p_3 s + p_4} = \\ = \frac{0.000104s^3 + 2.3167s^2 + 944.64s + 51422.4}{3.9996s^4 + 1164.7428s^3 + 66355.7952s^2 + 1297067.592s + 8142062.4}. \tag{42}$$

In Figure 17 are presented the transient responses of the automatic control system tuned using the polynomial method.

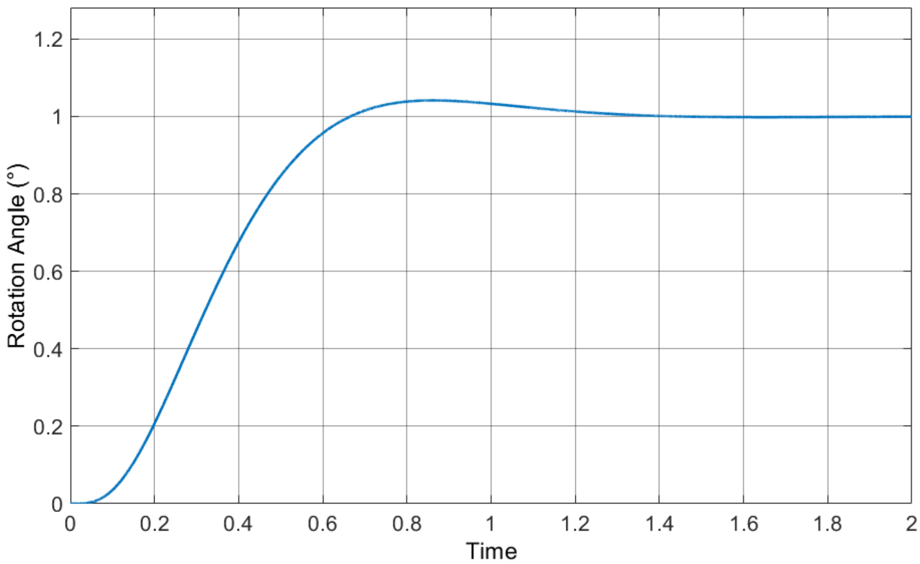

Figure 17. Transient response of the automatic control system tuned using the polynomial method.

As a result of the simulation, the following system performance was recorded: rise time $t_r = 0.58$ s, overshoot $d = 6.30$ %, settling time $t_s = 0.58$ s. and deviations $n = 1$ s.

4. Conclusions

This study demonstrated the design and implementation of a cascade control system for a DC servomotor used in robotic arm applications. The research focused on tuning and optimizing controllers for both the inner and outer control loops, using methods such as the Maximum Stability Degree with Iterations and the Polynomial method.

The proportional controller in the outer loop, combined with the inner loop P controller, exhibited the best overall performance in terms of rise time ($t_r = 0.297$) and settling time ($t_s = 0.321$ s). This configuration proved particularly effective for systems with astatism, offering rapid, and robust responses to both reference and disturbance signals.

The inner loop's performance with a PI controller demonstrated significant improvement in transient behavior, achieving better system stability and reduced steady-state error compared to the P controller.

The outer loop's use of PI and PID controllers achieved satisfactory results but introduced overshoots in transient responses due to the inherent characteristics of the system. Despite this, the PID controller yielded the most accurate positioning, making it suitable for applications requiring high precision.

The polynomial method was successfully applied to tune the controller in the outer loop, providing enhanced accuracy in system performance. This method offered flexibility in adjusting system dynamics, ensuring precise tuning for desired response characteristics.

The research highlights the practical benefits of implementing a cascade control system in robotic applications, demonstrating its ability to reject disturbances effectively. Although the current two-loop control system provides satisfactory performance in terms of stability and response time, further improvements can be achieved by introducing a third control loop to regulate the rotational speed of the motor. This additional loop would allow the output shaft angle of the servomotor to change at different speeds and minimize speed fluctuations caused by external disturbances or load variations.

Acknowledgments: This work was supported by the subproject 02.04.04 „Innovations in Biomedical Engineering: Advanced Technologies and Applications for Data Acquisition, Processing, and Analysis".

Conflicts of Interest: The authors declare no conflict of interest.

References

1. Wang, Y.; Wang, Y.; Mushtaq, R.; Wei, Q. Advancements in Soft Robotics: A Comprehensive Review on Actuation Methods, Materials, and Applications. *Polymers* 2024, 16(8), 1087.
2. Kim, S.; Laschi, C.; Trimmer, B. Soft robotics: a bioinspired evolution in robotics. *Trends Biotechnol.* 2013, 31(5), pp. 287-294.
3. Rus, D.; Tolley, M. T. Design, fabrication and control of soft robots. *Nature* 2015, 521, pp. 467-475.
4. Stavridis, S.; Falco, P.; Doulgeri, Z. Pick-and-place in dynamic environments with a mobile dual-arm robot equipped with distributed distance sensors. In: *IEEE-RAS 20th International Conference on Humanoid Robots (Humanoids)*. 2021, Munich, Germany, 19-21 July 2021.
5. Navarro, S.E.; Mühlbacher-Karrer, S.; Alagi, H.; Zangl, H.; Koyama, K.; Hein, B.; Duriez, C.; Smith, J. R. Proximity Perception in Human-Centered Robotics: A Survey on Sensing Systems and Applications. *IEEE Transactions on Robotics* 2022, 38(3), pp. 1599-1620.
6. Xie, D.; Chen, L.; Liu, L.; Chen, L.; Wang, H. Actuators and Sensors for Application in Agricultural Robots: A Review. *Machines* 2022, 10, 913.
7. Boussaada, D.; Chen, J.; Bonnet, C.; Niculescu, S.I.; Chen, J. PID control design for first-order delay systems via MID pole placement: Performance vs. robustness. *Automatica* 2022, 137, pp. 110-102.
8. Tarczewski, T.; Skiwski, M.; Niewiara, L.J.; Grzesiak, L.M. High-performance PMSM servo-drive with constrained state feedback position controller. *Bulletin of the polish academy of sciences technical sciences* 2018, 66(1), pp. 49-58.
9. Izvoreanu, B. The Iterative Algorithm of Tuning Controllers to the Model Object with Advance Delay and Inertia Second Order. In: *Proceedings of the 10-th International Conference on Development and Application Systems DAS-2010*. 22-24 May 2010, Suceava. pp. 111-115.
10. Kim, D. P. *Teoria avtomaticheskogo upravlenia*. T. 1. *Lineinye sistemy*. Fizmatlit, Moscow, 2003, 288 p.
11. Kiм, D. P.; Dmitrieva, N. D. *Sbornik zadach po teorii avtomaticheskogo upravlenia. Lineinye sistemy*. Fizmatlit, Moskva, 2007, 167 p.

12. Izvoreanu, B. *Automation Systems Engineering. Course material.* Technique-TUM, Chisinau, RM, 2024, 337 p. [in Romanian].
13. Electrical4u: *RL circuit transfer function time constant*, © 2024 (accessed 05.06.2024). Available online: https://www.electrical4u.com/rl-circuit-transfer-function-time-constant-rl-circuit-as-filter/. (accessed on 02.11.2024).
14. Isd-Soft: *Tuning a PID regulator*. © 2023 (accessed 02.06.2024). Available online: https://isd-soft.com/tech_blog/tuning-pid-regulator/ (accessed on 05.11.2024).
15. Dumitrache, I. *Automatic control engineering*. Politehnica Press, Bucharest, Romania, 2016, 407 p. [in Romanian].
16. Ahmed, A.S.; Marzog, H.A.; Abdul-Rahaim, L. A. Design and implement of robotic arm and control of moving via IoT with Arduino ESP32. *International Journal of Electrical & Computer Engineering* 2021 11(5), pp. 101-110.
17. Mhawesh, M.A. Performance comparison between variants PID controllers and unity feedback control system for the response of the angular position of the DC motor. *International Journal of Electrical and Computer Engineering* 2021, 11(1), pp. 802-814.
18. Dewi, T.; Nurmaini, S.; Risma, P.; Oktarina, Y.; Roriz, M. Inverse kinematic analysis of 4 DOF pick and place arm robot manipulator using fuzzy logic controller. *International Journal of Electrical &Computer Engineering* 2020, 10(2), pp. 1376-1378.
19. Borase, R.P.; Maghade, D.K.; Sondkar, S.Y.; Pawar, S.N. A review of PID control, tuning methods and applications. *International Journal of Dynamics and Control* 2021, 9, pp. 818–827.
20. Chotikunnan, P.; Chotikunnan, R. Dual Design PID Controller for Robotic Manipulator Application. *Journal of Robotics and Control* 2023, 4(1), pp. 23-34.
21. Ma'arif, A.; Setiawan, N. R. Control of DC motor using integral state feedback and comparison with PID: simulation and Arduino implementation. *Journal of Robotics and Control (JRC)* 2021, 2(5), pp. 456-461.
22. Koca, Y.B.; Aslan, Y.; Gökçe, B. Speed Control Based PID Configuration of a DC Motor for An Unmanned Agricultural Vehicle. In: *8th International Conference on Electrical and Electronics Engineering (ICEEE)*. Antalya, Turkey, 09-11 April 2021. pp. 117-120.
23. Ramadhani, N.; Ma'arif, A.; Çakan, A. Implementation of PID Control for Angular Position Control of Dynamixel Servo Motor. *Control Systems and Optimization Letters* 2024, 2(1), pp 8-14.
24. Moraru, D. Tuning method of automatic controllers to object models with second order advance-delay and dead time. *Acta et Commentationes Exact and Natural Sciences* 2023, 2(16), pp. 78–88.
25. Zagarii, G. I., Shubladze, A. M. *Sintez sistem upravlenia na osnove kriteria maximalnoi stepeni ustoichivosti*. Energoatomizdat, Moskva, 1998, 198 s.

Citation: Moraru, D.; Fiodorov, I.; Izvoreanu, B.; Cojuhari, I. Cascade control algorithm of the robotic arm's servomotor. *Journal of Engineering Science* 2024, XXXI (4), pp. 124-141. https://doi.org/10.52326/jes.utm.2024.31(3).01.

Publisher's Note: JES stays neutral with regard to jurisdictional claims in published maps and institutional affiliations.

Copyright:© 2024 by the authors. Submitted for possible open access publication under the terms and conditions of the Creative Commons Attribution (CC BY) license (https://creativecommons.org/licenses/by/4.0/).

Submission of manuscripts: jes@meridian.utm.md